

Measurement of preheat in aluminium target in indirect drive using the SGIII prototype facilities

C Zhang^{1,2}, Z B Wang³, H Liu³, X S Peng³, F Wang³, Y K Ding³ and J Zheng^{1,2}

¹ CAS Key Lab of Basic Plasma Physics, Hefei, Anhui 230026, P. R, China

² Department of modern physics, University of Science and Technology of China, Hefei, Anhui 230026, P. R. China

³ Research Center of Laser Fusion, China Academy of Engineering Physics, Mianyang, Sichuan 621900, P. R. China

E-mail: zcph@mail.ustc.edu.cn

Abstract. The velocity interferometer system for any reflector (VISAR) is used to demonstrate preheat effect in aluminium in indirect drive. The rear surface motion prior to shock front was observed and compared with a multi-group calculation. By properly adjusting the hard x-ray portion of the radiation source, the calculated rear surface motion fits well with the experimental results, which gives us confidence to predict the preheated temperature of the sample by hard x-rays. Further, the effect of hohlraum geometry is compared and discussed experimentally. The result suggests gas-filled hohlraum or hohlraum with low Z substrates should be considered to further reduce preheating.

1. Introduction

The study of sample preheating is an inescapable issue during the equation of state measurement. For the indirect drive scheme, the hohlraum provides a radiation source with adequate spatial uniformity and compresses samples into high energy density states with strong shocks [1]. However, some high energy photons like M-band x-rays are generated in the hohlraum [2]. These photons would penetrate deep into the target and heat the sample before shocks arrival. This preheating may play a role of violation and degenerate the diagnostic accuracy [3]. As a result, the experimental diagnostics of sample preheating and a way to reduce it is of great importance.

In this article, the preheating of aluminum is investigated by using the VISAR system. The rear surface velocity of the sample is accurately measured. The results are verified by using multi-group hydrodynamic simulation [4], which gives a relatively good description for the preheating phenomenon. Besides, a special designed hohlraum is tested to control the preheating for the sample. The effect of hohlraum geometry on the sample preheating is experimentally compared and discussed. The comprehensive analysis suggests gas fill hohlraum or hohlraum with low Z substrate is needed to prevent plasma from convergence and to further reduce preheating.

2. Experimental setup

The configuration of the experiment is illustrated in figure 1 (a). It is performed in the SGIII prototype facility [5], which has eight Nd: glass beams operating at 1.053 μm . In our experiment, we use the 3ω



mode. The continuous phase plate (CPP) technique is applied to smooth out each beam. The laser focal spot has a full-width-half-maximum (FWHM) around 0.6 mm. The pulse width is 3 ns with the total energy of 5.2 kJ, resulting in the laser spot intensity of 1×10^{14} W/cm².

A gold cylinder hohlraum with the size of 1.5 mm in diameter and 1.2 mm in length is placed in the center of the vacuum chamber. The hohlraum has a laser entrance hole (LEH) in the upper surface of 0.9 mm and a diagnostic hole (DH) in the bottom of 0.7 mm \times 0.4 mm. The eight laser beams are simultaneously delivered into the hohlraum from the LEH. The radiation temperature of the source is measured by using a multichannel soft x-ray spectrometer (SXS) [6] from the 20° azimuth angle with respect to the hohlraum axis. A set of flat-response x-ray detector (FXRD) [7] array is equipped to verify the total flux diagnostics.

A planar aluminum with a thickness of 35 μ m is attached to the DH, which is the preheating sample in our experiment. The observed rear surface is defined as the critical density for the probe beam, which has a wavelength of 532 nm. It is the location where reflection occurs. Through a reflective mirror assembled on the target with designed angle, the observation direction of VISAR is perpendicular to the aluminum surface and it has a view of the whole aluminum sample. The preheating effect of the sample is mainly diagnosed through this VISAR system. The probe beam is reflected from the aluminum surface and transmitted into an interferometer system. Then the interference fringe is imaged onto the slit of an optical streak camera. The position of the image is adjusted so that its central part is observed to ensure the feasibility of one dimensional approximation in our experiment. The system enables a spatial resolution of 10 μ m and a temporal resolution of 20ps. The rear surface expansion due to preheat is obtained from the fringe shift. The sensitivities of the two channels are 2.35 km/s/fringe and 3.04 km/s/fringe, respectively. The detection threshold is 1/10 fringes and the minimum detectable velocity is around 0.2 km/s. Since aluminum is widely used as a standard material in EOS measurements, the study could help us to specify the effect of preheating on EOS diagnostics.

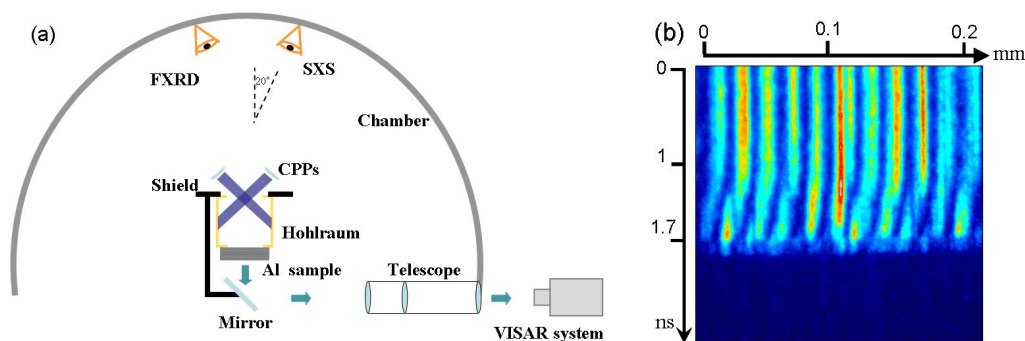


Figure 1 (a): Experimental setup is illustrated. (b): Image from VISAR measurement.

3. Experimental results and discussion

In our experiment, the contribution to preheating from hot electrons can be ignored because of the low intensity and the uniform laser spot. The laser plasmas interaction (LPI) processes are not effectively stimulated. Thus, the preheating mainly contributes from x-ray radiation transport.

3.1. Rear surface motion

The typical VISAR result is shown in figure 1 (b). The horizontal axis provides the spatial direction and the vertical one is the time axis. Time zero stands for the arrival of the main pulse. No movement is observed of the interference fringe before 1 ns due to low preheating level. However, between $t = 1$ ns to $t = 1.7$ ns, apparent shift occurs, indicating the motion of the sample's rear surface. After $t = 1.7$ ns, the shock breaks out from the rear surface. The released plasma becomes a good absorber for the probe beam, resulting in a sudden disappearance of the fringe. The velocity of the rear surface is deduced accordingly in figure 2 (a) and matches the simulation result from MULTI1D well. In our

simulation, we choose Theromos database [8] as the opacity tables and divide the photons into 35 groups. A factor of 0.82 is multiplied to the radiation temperature obtain by SXS in order to match the shock break-out time. This factor may represent the transport efficiency from the LEH to the DH. The spectrum we use in our simulation is constructed by a Planckian spectrum plus two Gaussian bumps centered at energy $E_1 = 1.4$ keV and $E_2 = 3.5$ keV, respectively. The former bump just locates near aluminum K-edge, which has a higher penetrability. The temporal evolution of the two bumps is illustrated in figure 2 (b). The fractions remain small before $t = 1$ ns, corresponding to a low preheating level in figure 1 (b) and figure 2 (a). After then both fractions increase notably, which probably results from the motion and convergence of gold plasma in the center of the hohlraum. With higher electron density and temperature, the emission of the piled up plasma tends to be stronger and more energy is converted into hard x-rays which shall enhance preheating.

According to the simulation, the highest preheating temperature of aluminum ahead of the shock is about 1800 K in our experiment, which is below aluminum's boiling point of over 2700 K. As a result, the state of the sample is still liquid. Further more, the reflectivity maintains high value before shocks. This phenomenon indicates the reflective surface should be in metallic state rather than plasma state, which is a strong absorber for the probe beam. Based on the above two facts, it is deduced the fringe shifts should be due to the rear surface motion instead of other factors, such as plasma expansion.

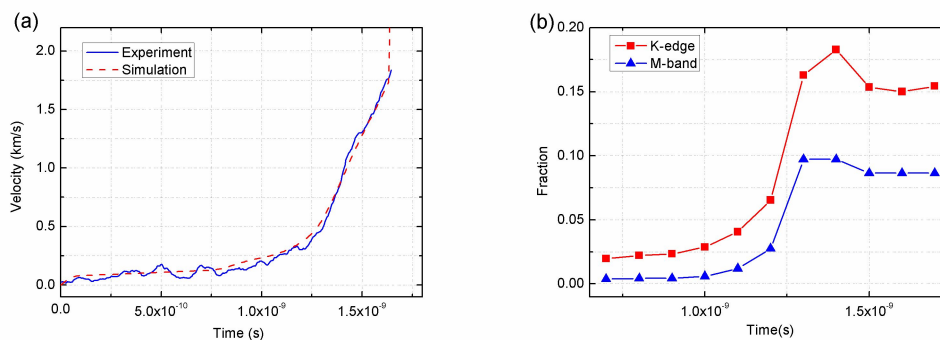


Figure 2 (a): the experimental result (blue curve) compared with simulation (dashed red). **(b):** the temporal evolution for the fractions of aluminum K-edge (red) and gold M-band (blue).

3.2. Effect of hohlraum geometry

In order to suppress preheating in the hohlraum, a special hohlraum is designed to shield the laser spot from the sample, as shown in figure 3 (a) and figure 3 (b). The special designed hohlraum contains a double-cylinder structure. The laser beams just lay within the turning corner of the two cylinders. This special geometric design serves to prevent the sample from “seeing” the laser spot directly.

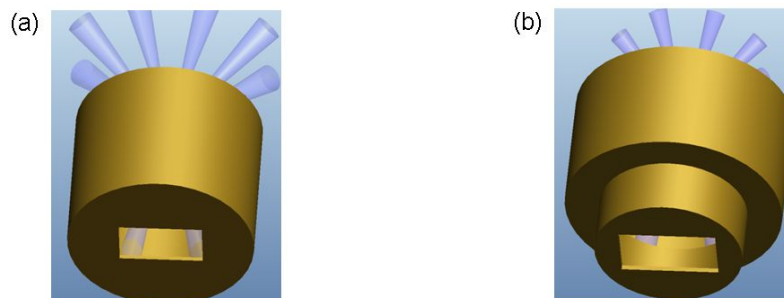


Figure 3 (a): the typical shape of a hohlraum design. **(b):** the special designed hohlraum, which contains a double-cylinder structures.

The resultant rear surface velocity and the predicted preheating temperature for different hohlraum designs are given in figure 4 (a) and figure 4 (b), respectively. The rise of velocity for the typical hohlraum is apparently much faster, which implies a stronger preheating level. The predicted temperature of the rear surface for the typical hohlraum is approximately twice the magnitude of the modified ones at the same time. However, sample preheat would last a longer time due to smaller source intensity and continuous plasma motion. The final preheat temperature is of the same order as the normal hohlraum. This result suggests additional improvements, such as low Z substrates in the hohlraum, are needed to further suppress preheating.

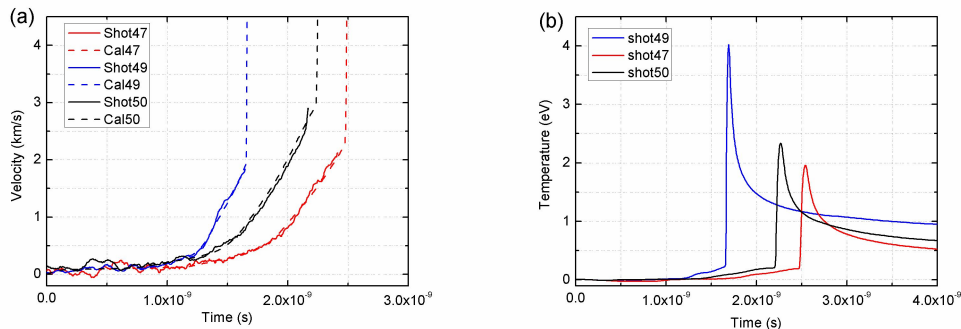


Figure 4 (a): the rear surface motion of different hohlraum designs. **(b):** the predicted temperature evolution for each shot. The typical hohlraum result is blue, while the special designed hohlraum is black and red.

4. Summary

We have investigated the preheating effect in indirect drive scheme in SGIII prototype facility. The rear surface velocity is measured using high sensitivity VISAR system. The phenomenon is reproduced by multi-group hydrodynamic simulation, which gives a good prediction for preheating studies. Besides, a suitable hohlraum design could reduce preheating to a lower level and current result implies there is still space to improve hohlraum designs.

References

- [1] Löwer Th, Sigel R, Eidmann K, Földes I B, Hüller S, Massen J, Tsakiris G D, Witkowski S, Preuss W, Nishimura H, Shiraga H, Kato Y, Nakai S and Endo T 1994 *Phys. Rev. Lett.* **72** 3186
- [2] McDonald J W, Suter L J, Landen O L, Foster J M, Celeste J R, Holder J P, Dewald E L, Schneider M B, Hinkel D E, Kauffman R L, Atherton L J, Bonanno R E, Dixit S N, Eder D C, Haynam C A, Kalantar D H, Koniges A E, Lee F D, MacGowan B J, Manes K R, Munro D H, Murray J R, Shaw M J, Stevenson R M, Parham T G, Van Wonterghem B M, Wallace R J, Wegner P J, Whitman P K, Young B K, Hammel B A and Moses E I 2006 *Phys. Plasmas.* **13** 032703
- [3] Rothman S D, Evans A M, Horsfield C J, Graham P and Thomas B R 2002 *Phys. Plasmas.* **9** 1721
- [4] Ramis R, Schmalz R and Meyer-Ter-Vehn J 1988 *Comp. Phys. Commu.* **49** 475
- [5] Li P, Jing F, Wu D S, Zhao R C, Li H, Lin H H and Su J Q 2012 *Proc. SPIE* **8433** 843317
- [6] Song T M, Yang J M and Yi R Q 2010 *High Power Laser and Particle Beams* **22**, 2017
- [7] Li Z C, Jiang X H, Liu S Y, Huang T X, Zheng J, Yang J M, Li S W, Guo L, Zhao X F, Du H B, Song T M, Yi R Q, Liu Y G, Jiang S E and Ding Y K 2010 *Rev. Sci. Instrum.* **81** 073504
- [8] Ivanov E M, Rozanov V B and Vergunova G A 2003 *Proc. of SPIE* **12** 79